

# OPTIMAL EFFICIENCY-POWER TRADEOFF FOR AN AIR MOTOR/COMPRESSOR WITH VOLUME VARYING HEAT TRANSFER CAPABILITY

**Andrew T. Rice and Perry Y. Li**  
Department of Mechanical Engineering  
University of Minnesota  
Minneapolis, Minnesota 55455  
Email: pli@me.umn.edu

## ABSTRACT

This paper presents the pressure-volume trajectories that yield the optimal trade-off between efficiency and power during the compression and expansion of air. These results could benefit applications such as compressed air energy storage where both high efficiency and power density are required. Earlier work established solutions for the simple case in which  $hA$ , the product of the heat transfer coefficient and heat transfer surface area, is constant. This paper extends that analysis by allowing  $hA$  to vary with air volume. Solutions to the constrained, non-linear optimization problem are developed utilizing the method of Lagrange multipliers and Karush-Kuhn-Tucker (KKT) conditions. It is found that the optimal trajectory takes the form “fast-slow-fast” where the fast stages are adiabatic and the temperature change during the slow stage is proportional to the inverse root of the  $hA$  product. A case study predicts a 60% improvement in power over the constant- $hA$  solution when both trajectories are run at 90% efficiency and  $hA = hA(V)$ . Compared to linear- and sinusoidal-shaped trajectories, also at 90% efficiency, power gains are expected to be around 500–1500%.

## 1 Introduction

Gas compression and expansion is common in many pneumatic and hydraulic systems. It is desired that such compression and expansion is both energy efficient and power-dense. An example would be compressed air energy storage. One such configuration proposed in [1], the Open Accumulator, consists of dual liquid and compressed air components. It can be operated pneumatically or hydraulically to take advantage of the high energy storage density of compressed air storage (about 20 times greater than hydraulic accumulators), and the high power den-

sity of conventional hydraulic accumulators. By operating them in concert, the accumulator pressure can also be maintained at a high level even as air mass depletes. Nevertheless, as with any compressed air storage concept, an efficient and powerful air motor/compressor is needed. These two criteria, efficiency and power, are coupled through the heat transfer characteristics of the system. Efficiency decreases when work is used to change the air temperature. To prevent temperature changes, high heat transfer (a rate) is required. Thus, the magnitude of the temperature change in the gas (i.e. efficiency) is related to the time allowed for heat transfer, which is determined by the overall speed of compression or expansion (i.e. power).

A common approach to the power vs efficiency tradeoff is the enhancement of the heat transfer. Suggested improvements include the insertion of elastomeric foams [2] into the air space or thin metallic strands bonded to a heat sink [3]. These features increase the surface area available for heat transfer, increase the thermal capacitance of the air space, and promote mixing. Foams, strands, fins, mesh (e.g. [4]), honeycomb, and other porous structures are most appropriate for piston-cylinder compressors/motors when a deformable liquid column is used as the piston [5]. A second approach is to incorporate multiple stages with intercooling [6]. A third approach is to control and optimize compression and expansion trajectories [7] [8] [9]. In these studies, calculus of variations is employed to optimize the work output during expansion with a given heating rate, as during the power stroke in an engine cylinder. Optimal piston trajectories for Otto and diesel cycles are determined in [10] [11]. A recent work by Sancken and Li [12] uses the method of Lagrange multipliers and corroborates the results of [7]. Sancken and Li determine that the optimal compression and expansion trajectories take the form adiabatic-isothermal-adiabatic where the isother-

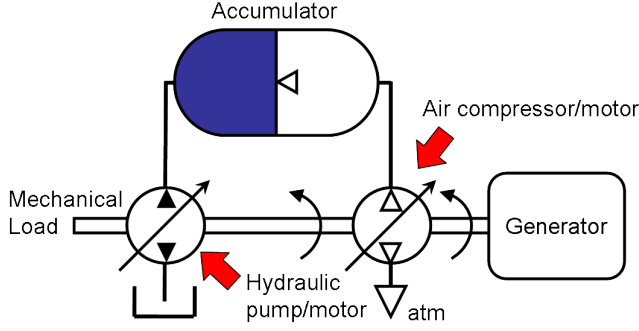


Figure 1. Schematic of the Open Accumulator system as described in [1].

mal temperature is equal to the root of the product of the initial and final temperatures. This paper takes the trajectory optimization approach; specifically, it extends the work by Sancken and Li.

In the analysis by Sancken and Li, the rate of heat transfer from the system is assumed to be directly proportional to the temperature difference between the gas and the environment. That is,  $hA$ , the product of the heat transfer coefficient and heat transfer surface area, is constant. Some studies suggest that over a limited operating range, this is an appropriate assumption [13] [14]; however, this is not true in general. The heat transfer coefficient,  $h$ , can be a complicated function of gas velocities [15] [16], temperature [17], unsteady flow features [18], boundary layer growth [19] [20], and other factors [21]. The surface area available for heat transfer,  $A$ , is typically a function of air volume. Of these influences on  $hA$ , air volume is one of the most accessible and important—increasingly so when the potential surface area changes dramatically over the cycle, as is the case with porous media and liquid piston [5]. For these reasons, the present work extends the results of [12] by allowing the  $hA$  product to vary as a function of air volume. Although still much simplified, this extension is a step forward since it captures some of the variable nature of  $hA$ . This variable nature is manifested in the solution: the modified optimal trajectory retains the same fast-slow-fast form, but the slow section depends explicitly on the  $hA$  product, whereas in the constant- $hA$  solution the slow section is an isotherm.

## 2 System model and problem statement

For the purposes of this paper, a system similar to that of the Open Accumulator concept is employed, as in [12] (figure 1), although much of the analysis is generally applicable. In this system, ambient air (assumed to be an ideal gas) at temperature and pressure  $T_0$  and  $P_0$  is compressed to a pressure  $P_c = rP_0$ ,  $r$  being the pressure compression ratio, and temperature  $T_c$ . During compression, heat,  $Q$ , is exchanged between the system and the environment at  $T_0$ , as determined by  $hA$  and the time-dependent pressure-volume trajectory:  $\zeta_c(t) = (P(t), V(t))$ . The com-

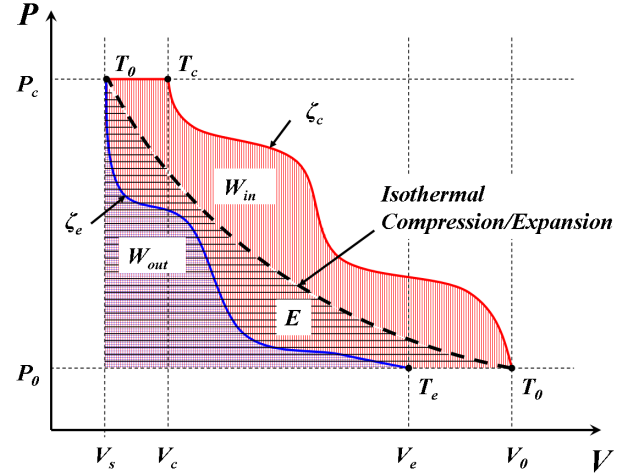


Figure 2. P-V diagram showing compression (red) and expansion (blue) trajectories. The shaded area under the curves represent the work input (red vertical lines) and work output (with added blue horizontal lines). Isothermal compression and expansion follows the dashed black trajectory. The total energy stored is marked by wide black horizontal lines. Reducing the area between  $\zeta_c$  and the isothermal curve increases compression efficiency. Reducing the area between the isothermal curve and  $\zeta_e$  increases expansion efficiency.

pressed air is moved into the accumulator and allowed to return to the ambient temperature isobarically, in line with the operation of the Open Accumulator concept. The assumption that the air has time to return to equilibrium with the environment before expansion is compatible with applications that require storage on the order of hours or longer, and is a conservative assumption in other cases. Thus, the total energy stored is equivalent to the work required to compress the air from  $P_0$  to  $P_c$  isothermally:

$$E \equiv nRT_0 \left[ \ln(r) - 1 + \frac{1}{r} \right]. \quad (1)$$

During regeneration, the compressed air is allowed to expand from initial conditions  $P_c$  and  $T_0$  to final pressure and temperature  $P_0$  and  $T_e$  within an air motor (or air compressor run in reverse). The expansion process is expressed as  $\zeta_e(t) = (P(t), V(t))$ . The entire process can be mapped onto a P-V diagram as in figure 2. In the following analysis friction is neglected and spatially uniform temperature and pressure are used for simplicity.

Pressure and volume are determined from the first law of thermodynamics and the equation of state for an ideal gas:

$$nc_v \dot{T} = q - P\dot{V} \quad \text{and} \quad P = \frac{nRT}{V} \quad (2)$$

where  $n$  is the quantity of air in moles,  $c_v$  is the constant volume specific heat of air,  $q$  is the heat transfer rate,  $P$  is the average

air pressure,  $V$  is the air volume,  $R$  is the universal gas constant, and  $T$  is the average air temperature. The specific heat,  $c_v$ , may be approximated as  $5R/2$  for a range of temperatures and will be considered constant. Let  $\gamma$  be the ratio of specific heats. Heat transfer is described by

$$q = hA(V)(T_0 - T) \quad (3)$$

where  $h$  is the heat transfer coefficient,  $A$  is the surface area available for heat transfer, and  $T_0$  is the heat sink/source temperature, assumed to isothermal and in equilibrium with the ambient. The  $hA$  product is a function of air volume.

For an arbitrary compression trajectory,  $\zeta_c$ , the work required to compress the air from  $(P_0, T_0)$  to  $(P_c, T_0)$  is

$$W_{\text{in}}(\zeta_c) = - \int_0^{t_c} (P(t) - P_0) \dot{V}(t) dt + nR(T_0 - T_c) \quad (4)$$

where  $t_c$  is the time it takes to compress the air from  $(P_0, T_0)$  to  $(P_c, T_c)$ . The second term describes isobaric cooling from  $(P_c, T_c)$  to  $(P_c, T_0)$ . Due to the heat up of the air during compression and subsequent cooling,  $W_{\text{in}}$  is larger than the stored energy  $E$ , as revealed in figure 2. For an arbitrary expansion trajectory,  $\zeta_e$ , the work provided when the air expands from  $(P_c, T_0)$  to  $(P_0, T_e)$  is

$$W_{\text{out}}(\zeta_e) = \int_0^{t_e} (P(t) - P_0) \dot{V}(t) dt \quad (5)$$

where  $t_e$  is the expansion time. Due to the cooling of the air during expansion,  $W_{\text{out}}$  is less than the stored energy  $E$ , as shown in figure 2. Work is nondimensionalized by  $E$  to obtain compression and expansion efficiencies:

$$\eta_c(\zeta_c) \equiv \frac{E}{W_{\text{in}}(\zeta_c)} \quad \text{and} \quad \eta_e(\zeta_e) \equiv \frac{W_{\text{out}}(\zeta_e)}{E}. \quad (6)$$

The rate at which energy is stored or regenerated is the power. Since  $E$  represents the total energy stored and  $W_{\text{out}}$  represents the total energy regenerated, the compression and expansion powers are defined, respectively, as

$$\text{Pow}_c(\zeta_c) \equiv \frac{E}{t_c} \quad \text{and} \quad \text{Pow}_e(\zeta_e) \equiv \frac{W_{\text{out}}(\zeta_e)}{t_e}. \quad (7)$$

The objective of this paper is to determine the Pareto optimal trajectory with respect to power and efficiency for compression from  $(P_0, T_0)$  to  $P_c$  and expansion from  $(P_c, T_0)$  to  $P_0$ , with a volume-dependent heat transfer rate  $Q = hA(V)(T_0 - T)$ . For a given efficiency, no other trajectory absorbs/provides more

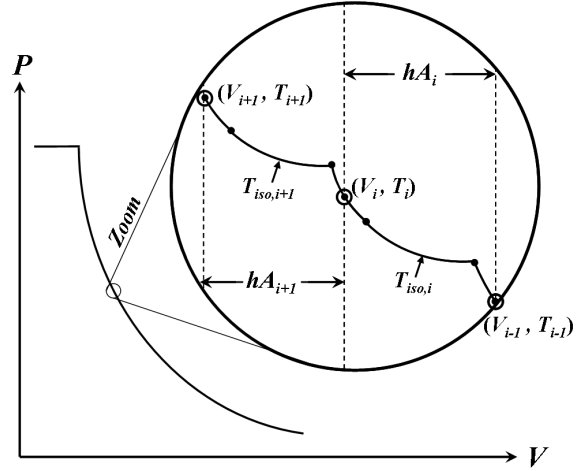


Figure 3. A compression trajectory is broken up into  $N$  adjacent volume intervals, each with a constant  $hA$ . Over each interval the optimal form of the compression trajectory is adiabatic-isothermal-adiabatic.

power than the Pareto optimal trajectory; for a given power, no other trajectory operates at higher efficiency. The optimization problem can be written as

$$\text{maximize } \eta(\zeta) \quad \text{s.t.} \quad \text{Pow}(\zeta) = \text{Pow}^* \quad (8)$$

where  $\text{Pow}^*$  is some prescribed power. Maximizing power for a given efficiency is an equivalent problem.

### 3 Optimal compression and expansion trajectories

The following steps address the problem for compression only; however, the expansion problem may be solved in the same manner.

1. Consider an arbitrary compression problem with initial volume  $V_0$ . Assuming  $hA$  is a function of air volume, the volume regime over which compression takes place may be discretized into  $N$  constant- $hA$  intervals:

$$hA = (hA)_i \quad \text{for } V_{i-1} \geq V > V_i \quad \forall i = 1, 2, \dots, N \quad (9)$$

where the  $V_i$ 's represent the transition volumes at which the  $hA$  product changes to a new value as in figure 3. Over each constant- $hA$  volume interval and for given initial and final pressures and volumes, Sancken and Li prove that the optimal trajectory with respect to work and time takes the form adiabatic-isothermal-adiabatic (AIA) [12]. To prove this, they propose that any curve may be uniformly approximated by a series of adiabatic and isothermal steps. The work and time for a sequence AIA is compared to the work and

time for a sequence Isothermal-Adiabatic-Isothermal (*IAI*) where the total compression ratios are the same. The authors demonstrate that *AIA* indeed takes less time than *IAI* with equal work. The series of adiabatic and isothermal steps can then be collapsed into a single *AIA* process by progressively replacing every occurrence of *IAI* with *AIA* (e.g. *IAIAIA*  $\Rightarrow$  *AIAAIA*  $\Rightarrow$  *AIATA*  $\Rightarrow$  *AAIAA*  $\Rightarrow$  *AIA*).

- For the repeating *AIA* sequence proposed above, the input work can be uniquely described by the temperatures of each isotherm,  $T_{\text{iso},i}$ , and temperatures at each transition volume,  $T_i$ :

$$\frac{W_{\text{in}}}{nR} = \gamma \frac{T_c - T_0}{\gamma - 1} - \sum_{i=1}^N T_{\text{iso},i} \ln \left[ \frac{V_i}{V_{i-1}} \left( \frac{T_{i-1}}{T_i} \right)^{\frac{1}{1-\gamma}} \right] + T_0 \left( \frac{1}{r} - 1 \right). \quad (10)$$

The compression time consists of the time required for the isothermal stages only; for a non-zero  $hA$ , the adiabatic stages must be instantaneous. Also, the final isobaric cooling stage does not contribute to the compression time because it takes place inside the accumulator, not the compressor. Thus, the compression time is found by integrating the first law from equation (2), when  $\dot{T}$  is zero. As with  $W_{\text{in}}$ , the compression time can be written as a function of the isothermal and transition temperatures of each constant- $hA$  volume interval:

$$\frac{t_c}{nR} = \sum_{i=1}^N \frac{T_{\text{iso},i}}{(hA)_i (T_0 - T_{\text{iso},i})} \ln \left[ \frac{V_i}{V_{i-1}} \left( \frac{T_{i-1}}{T_i} \right)^{\frac{1}{1-\gamma}} \right]. \quad (11)$$

- Reformulate the optimization problem formulation (8) using the equations for input work and compression time:

$$\begin{aligned} &\text{minimize} && W_{\text{in}}(T_{\text{iso},1}, T_1, \dots, T_{\text{iso},N}, T_N) \\ &\text{subject to} && t_c(T_{\text{iso},1}, T_1, \dots, T_{\text{iso},N}, T_N) = t_c^* \\ &&& T_i \leq \max(T_{\text{iso},i}, T_{\text{iso},i+1}) \quad \forall i = 1, \dots, N, \\ &&& T_i \geq \min(T_{\text{iso},i}, T_{\text{iso},i+1}) \quad \forall i = 1, \dots, N. \end{aligned} \quad (12)$$

Efficiency and power from the original problem statement (8) are transformed to work and time using equations (6) and (7). The temperature constraints force transition temperatures to lie between adjacent isothermal temperatures. Ignoring these constraints causes ambiguity when performing the Lagrange multiplier method to determine stationary points. The Karush-Kuhn-Tucker (KKT) conditions formalize the first order optimality conditions and provide a system of differential equations. Solutions to these equations satisfy stationarity conditions, primal and dual feasibility, and com-

plementary slackness. The stationarity conditions are

$$\begin{aligned} &nR \ln \left[ \frac{V_i}{V_{i-1}} \left( \frac{T_{i-1}}{T_i} \right)^{\frac{1}{1-\gamma}} \right] \\ &\quad \times \left( \frac{\lambda T_0}{(hA)_i (T_0 - T_{\text{iso},i})^2} - 1 \right) \\ &= \frac{\partial}{\partial T_{\text{iso},i}} [\mu_i \max(T_{\text{iso},i}, T_{\text{iso},i+1})] \\ &- \frac{\partial}{\partial T_{\text{iso},i}} [\nu_i \min(T_{\text{iso},i}, T_{\text{iso},i+1})] \quad \forall i = 1, \dots, N \end{aligned} \quad (13)$$

and

$$\begin{aligned} &T_{\text{iso},i} \left( 1 - \frac{\lambda}{(hA)_i (T_0 - T_{\text{iso},i})} \right) \\ &- T_{\text{iso},i+1} \left( 1 - \frac{\lambda}{(hA)_{i+1} (T_0 - T_{\text{iso},i+1})} \right) \\ &= \frac{T_i (1 - \gamma)}{nR} (\nu_i - \mu_i) \quad \forall i = 1, \dots, N. \end{aligned} \quad (14)$$

The Lagrange multipliers  $\lambda$ ,  $\nu_i$ , and  $\mu_i$  correspond to the constraints in (12):

$$\begin{aligned} \mu_i [T_i - \max(T_{\text{iso},i}, T_{\text{iso},i+1})] &= 0 \\ \nu_i [T_i - \min(T_{\text{iso},i}, T_{\text{iso},i+1})] &= 0 \end{aligned} \quad (15)$$

with  $\mu_i \geq 0$  and  $\nu_i \geq 0$  for all  $i = 1, 2, \dots, N$ .

- Consider when  $N \rightarrow \infty$ . Since  $hA(V)$  is a differentiable function, the differences in  $hA$  and isothermal temperature between adjacent intervals become arbitrarily small

$$T_{\text{iso},i} - T_{\text{iso},i+1} \rightarrow 0 \quad \text{and} \quad (hA)_i - (hA)_{i+1} \rightarrow 0. \quad (16)$$

Given these, the left hand side of equation (14) also goes to zero, forcing  $\mu_i \rightarrow \nu_i$ . As defined in equation (15), either  $\mu_i$  or  $\nu_i$  must equal zero (representing an active constraint) for each interval. Thus, as the continuous case is approached, the effect of individual constraints are diminished and all Lagrange multipliers tend toward zero, except  $\lambda_c$  in which case equation (13) reduces to

$$(hA)_i (T_{\text{iso},i} - T_0)^2 = T_0 \lambda_c \quad \forall i = 1, \dots, N \quad (17)$$

and as a function of volume, to

$$hA(V) (T - T_0)^2 = T_0 \lambda_c. \quad (18)$$

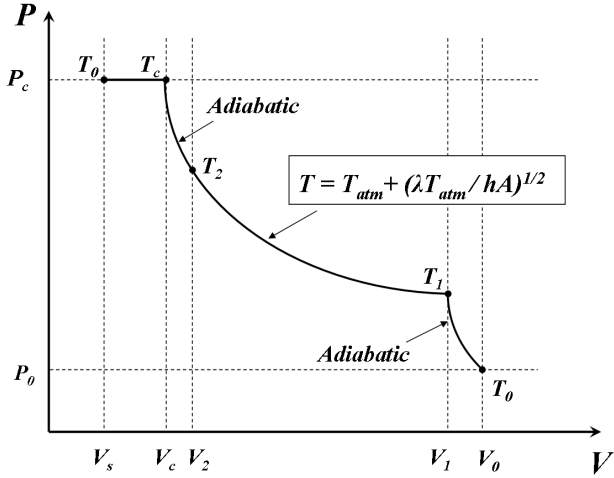


Figure 4. Optimal compression for a continuously varying  $hA$  product consists of three stages: adiabatic compression;  $hA$ -dependent compression; adiabatic compression. The slow  $hA$ -dependent curve is determined by the parameter  $\lambda_c$ . After the air is moved to the accumulator, the air volume is further reduced by isobaric cooling.

It is observed that in the continuous form, the AIA sequence has been smoothed into the curve defined by equation (18). All interior adiabatic bursts are absorbed; however, the initial and final adiabatic sections are not negligible since the curve defined by equation (18) does not necessarily intersect the prescribed initial and final temperatures. Thus, the form of the optimal compression trajectory is known. It consists of three stages: an initial adiabatic jump, an  $hA$ -dependent stage according to equation (18), and a final adiabatic jump, as in figure 4.

5. Reformulate expressions for work and time based on the discovered form of the optimal trajectory. Incorporating equation (18) allows work and time to be written as functions of  $T_c$  and  $\lambda_c$  only. Let the volume and temperature at which the trajectory changes from adiabatic compression to  $hA$ -dependent compression be  $V_1$  and  $T_1$ . Let the volume and temperature at which the trajectory changes from  $hA$ -dependent compression to adiabatic compression be  $V_2$  and  $T_2$ . These transition states,  $V_1$ ,  $T_1$ ,  $V_2$ , and  $T_2$  are themselves dependent on  $\lambda_c$  and  $T_c$ . Then from the definition of  $W_{in}$ , (4),

$$\frac{W_{in}}{nR} = \frac{\gamma(T_c - T_0)}{\gamma - 1} - \frac{T_2 - T_1}{\gamma - 1} + T_0 \ln \left( \frac{V_1}{V_2} \right) - \sqrt{T_0 \lambda_c} \int_{V_1}^{V_2} \frac{dV}{V \sqrt{hA(V)}} - T_0 \left( 1 - \frac{1}{r} \right) \quad (19)$$

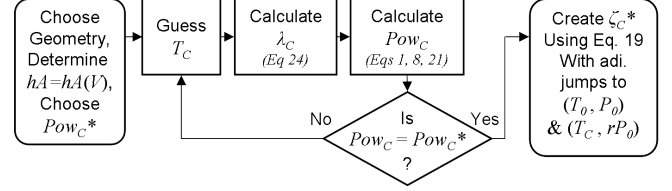


Figure 5. Determining the optimal trajectory for a given power.

and by integrating the first,

$$\frac{t_c}{nR} = - \int_{V_1}^{V_2} \frac{dV}{V hA(V)} - \sqrt{\frac{T_0}{\lambda_c}} \int_{V_1}^{V_2} \frac{dV}{V \sqrt{hA(V)}} + \frac{1}{2(\gamma - 1)} \left[ \frac{1}{hA(V_1)} - \frac{1}{hA(V_2)} \right]. \quad (20)$$

As before, the adiabatic stages are instantaneous and do not contribute to the compression time.

6. Plug the new formulations for work and time into the problem statement (8):

$$\begin{aligned} &\text{minimize } W_{in}(T_c, \lambda_c) \\ &\text{subject to } t_c(T_c, \lambda_c) = t_c^*. \end{aligned} \quad (21)$$

With only an equality constraint, the Lagrange multiplier method may be used. It yields

$$\frac{\partial W_{in}}{\partial \lambda_c} + \beta \frac{\partial t_c}{\partial \lambda_c} = 0 \quad \text{and} \quad \frac{\partial W_{in}}{\partial T_c} + \beta \frac{\partial t_c}{\partial T_c} = 0 \quad (22)$$

where  $\beta$  is a new Lagrange multiplier. Eliminating  $\beta$  yields a single equation relating  $T_c$  and  $\lambda_c$ :

$$\frac{\partial t_c}{\partial \lambda_c} \frac{\partial W_{in}}{\partial T_c} = \frac{\partial t_c}{\partial T_c} \frac{\partial W_{in}}{\partial \lambda_c}. \quad (23)$$

Equation (23) in addition to the constraint  $t_c = t_c^*$  form a system of two equations and two unknowns which may be solved for the optimal  $T_c$  and  $\lambda_c$ .

The optimal trajectory is constructed using equation (18) with  $\lambda_c$  to establish the interior compression stage and adiabats passing through  $(T_0, P_0)$  and  $(T_c, rP_0)$  to form the two outer stages. This solution is similar to the constant- $hA$  case derived by Sancken and Li in which the form is adiabatic-isothermal-adiabatic, but the temperature of the isothermal stage is independent of  $hA$ . Figure 5 summarizes the procedure when a power constraint is specified.

It should be noted that instantaneous adiabatic compression is not possible in real-life applications. Nevertheless, as reported

in the paper by Sancken and Li, assigning a finite compression rate to the adiabatic stages on the order of the fastest compression rate during the slow stage has a minimal effect at high efficiencies [12]. It should also be noted that the Lagrange multiplier method finds stationary points—not necessarily minima. That the proposed solution is not the worst case will become obvious in the case study! Additionally, perturbing  $\lambda_c$  or  $T_3$  reduces performance, indicating that the solution is, at least, locally optimal.

**Theorem 1. (Compression)** Let  $P_0$  and  $T_0$  be ambient pressure and temperature. Consider an ideal gas compressed from  $(P_0, T_0)$  to  $(rP_0, T_c)$  with  $r > 1$ . The compression trajectory,  $\zeta_c^*$ , is achieved by maintaining

$$hA(V)(T - T_0)^2 = \lambda_c T_0$$

where  $\lambda_c$  is a constant parameter and  $hA$  is a differentiable function of air volume. Instantaneous adiabatic jumps connect the  $hA$ -dependent curve to the initial and final states. The work input and compression time are functions of  $T_c$  and  $\lambda_c$ , related by

$$\frac{\partial t_c}{\partial \lambda_c} \frac{\partial W_{in}}{\partial T_c} = \frac{\partial t_c}{\partial T_c} \frac{\partial W_{in}}{\partial \lambda_c}.$$

The trajectory  $\zeta_c^*$  is Pareto optimal with respect to work and time. There does not exist a compression trajectory,  $\zeta_c$ , under identical conditions such that

$$W_{in}(\zeta_c) < W_{in}(\zeta_c^*) \quad \text{and} \quad t_c(\zeta_c) < t_c(\zeta_c^*).$$

**(Expansion)** Let  $P_0$  and  $T_0$  be ambient pressure and temperature. Consider an ideal gas expanded from  $(rP_0, T_0)$  to  $(P_0, T_e)$  with  $r > 1$ . The expansion trajectory,  $\zeta_e^*$ , is achieved by maintaining

$$hA(V)(T - T_0)^2 = \lambda_e T_0$$

where  $\lambda_e$  is a constant parameter and  $hA$  is a differentiable function of air volume. Instantaneous adiabatic jumps connect the  $hA$ -dependent curve to the initial and final states. The work out and expansion time are functions of  $T_e$  and  $\lambda_e$ , related by

$$\frac{\partial t_e}{\partial \lambda_e} \frac{\partial W_{out}}{\partial T_e} = \frac{\partial t_e}{\partial T_e} \frac{\partial W_{out}}{\partial \lambda_e}.$$

The trajectory  $\zeta_e^*$  is Pareto optimal with respect to work and time. There does not exist an expansion trajectory,  $\zeta_e$ , under identical conditions such that

$$W_{out}(\zeta_e) > W_{out}(\zeta_e^*) \quad \text{and} \quad t_e(\zeta_e) < t_e(\zeta_e^*).$$

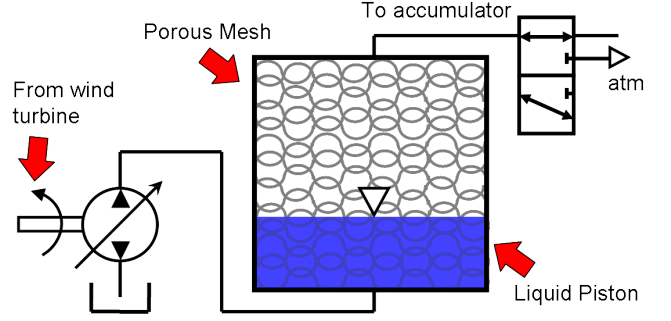


Figure 6. Schematic of the compressor with liquid piston and porous mesh for the case study.

#### 4 Case study

Offshore wind is becoming more prevalent as a renewable energy source. One issue with wind power is that the wind does not necessarily blow at the same time power is required by consumers. A promising remedy is energy storage. Suppose the Open Accumulator infrastructure is used to capture and store energy as efficiently as possible for a specific geometry and volume-dependent heat transfer function. How might the piston trajectory look with a 1 MW power requirement? Let the compression chamber geometry be that of a 12 m<sup>3</sup> cylindrical drum, with an aspect ratio of unity. To improve the heat transfer, uniformly fill the chamber with a perfectly conducting metallic mesh bonded to isothermal chamber walls and use a liquid piston with a direct liquid-to-air interface as in figure 6. During compression the liquid will gradually fill the compression chamber and submerge the porous mesh surface area as it reduces air volume. If, for simplicity, it is assumed that  $h$  is 100 W/m<sup>2</sup>-K and constant, then the  $hA$  product will vary with air volume as

$$hA(V) = h \left[ \left( \frac{4V(1-\epsilon)}{Dd\epsilon} + \pi D \right) \frac{4V}{\pi\epsilon D^2} + \frac{\pi D^2}{2} \right] \quad (24)$$

where  $\epsilon$  is the porosity of the mesh,  $d$  is the diameter of a single strand of the mesh,  $D$  is the diameter of the chamber, and  $V$  is the instantaneous volume of air in the chamber. Let porosity be 99.5% and the wire diameter be 80  $\mu$ m. Let the pressure compression ratio be 350. Following the flow chart in figure 5 will determine the optimal trajectory. The power is specified to be 1 MW. Selected outputs are tabulated below.

$Pow_c$	$1.00 \times 10^6$ W	$\eta_c$	0.803
$t_c$	5.88 s	$W_{in}$	$7.33 \times 10^6$ J
$T_0$	298 K	$T_1$	309 K
$T_2$	379 K	$T_c$	539 K
$\lambda_c$	$1.04 \times 10^5$ W		

Assuming the same geometry and heat transfer characteristics

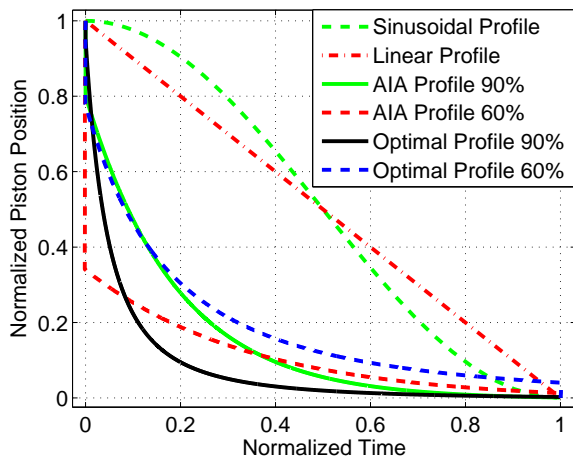


Figure 7. Sample profiles of the optimal trajectory for various efficiencies. Volume, normalized by the maximum volume, is shown as a function of time, scaled by total compression time. Sinusoidal, linear, and AIA trajectories are provided for comparison.

described by equation (24), sample results are provided to assist in visualizing the process. Figure 7 displays normalized volume trajectories throughout the compression cycle for two different efficiencies: 90% and 60%. They each have a instantaneous stage, a slow stage, and a final instantaneous stage. Higher efficiency trajectories have shorter adiabatic compression stages, as can be seen in the figure. Recall that isothermal compression is the most efficient. Adiabatic-isothermal-adiabatic (AIA) volume trajectories are plotted in figure 7 as well using the same efficiencies. When the  $hA$  product is constant, the AIA trajectory is optimal. When  $hA$  is not constant, as in this case study, the AIA trajectory absorbs less power than the variable- $hA$  optimal trajectory at the same efficiency. Also plotted for purposes of comparison are linear and sinusoidal profiles. Conventional crank driven pistons often use sinusoidal trajectories. The optimal profile intuitively looks more appropriate than sinusoidal or linear profiles for the chosen function of  $hA$ . At low pressures, when the required work is minimal, compress as fast as possible. Once the temperature begins to rise, slow down and take advantage of the still-large heat transfer surface area. As compression progresses, the surface area (and therefore heat transfer) diminishes, and eventually it is best to forgo the slow compression and push on to the final pressure as fast as possible. The same reasoning applies to expansion, but in reverse order.

Figure 8 demonstrates the benefits of the optimal compression trajectory over ad hoc approaches. In the figure, compression efficiency is plotted against power absorbed. At any efficiency, the optimal trajectory absorbs more power than any other trajectory. For example, at 90% efficiency, compression via the optimal trajectory absorbs over 5 times the power of sinusoidal compression and over 15 times the power of linear compression. Compared to the adiabatic-isothermal-adiabatic solution, the op-

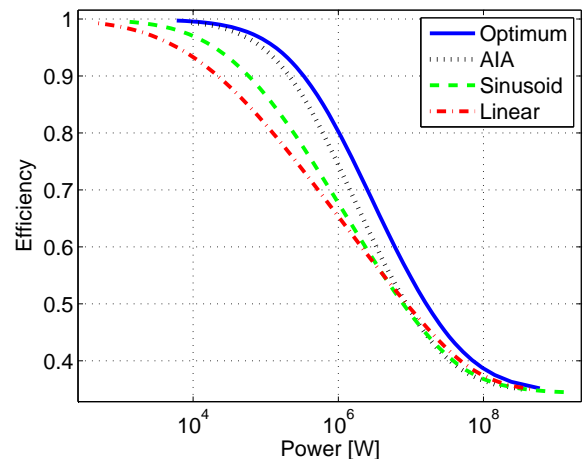


Figure 8. Compression efficiency vs power. There is no other trajectory that allows more power to be absorbed at a given efficiency than the optimal trajectory. Sinusoidal, linear, and AIA trajectories are provided for comparison.

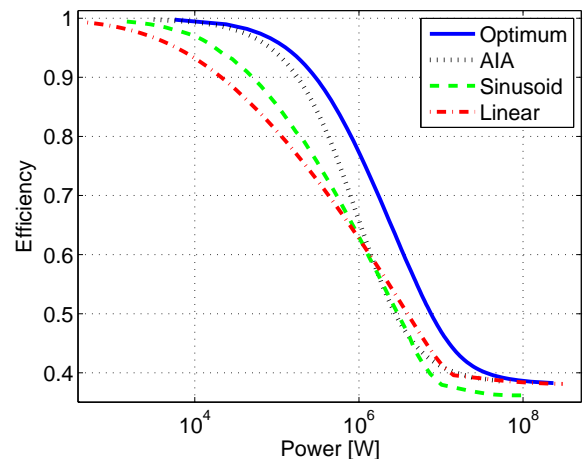


Figure 9. Expansion efficiency vs power. There is no other trajectory that allows more power to be produced at a given efficiency than the optimal trajectory. Sinusoidal, linear, and AIA trajectories are provided for comparison.

timal trajectory absorbs 60% more power, also at 90% efficiency. It needs to be emphasized, however, that these numbers are for a specific case. Figure 9 plots expansion efficiency against power output. Again, the curve representing optimal expansion demonstrates superior power for any efficiency.

## 5 Conclusions

The ability to compress and expand air at high power while maintaining high efficiency is a critical objective in the design and development of air motor/compressors. It has been shown

that significant gains are made by controlling the pressure-volume trajectories of the gas. Previous work has demonstrated these gains under the assumption of a constant  $hA$  product. This paper extends that work to encompass situations where  $hA$  varies with air volume. The optimal trajectory was found to take a three stage form in which a middle stage is determined by the  $hA$  product and the end stages are adiabatic. By employing an optimized trajectory for a simple case,  $5\times$  to  $15\times$  power gains are predicted over sinusoidal and linear trajectories at 90% efficiency.

In this analysis key assumptions were made that need to be reconsidered for practical applications. Examples include a instantaneous compression speed and a negligence of friction. The difficulty of designing a controller to track the optimal trajectory based on the real-time value of  $hA$  is another issue that will need to be addressed in future work. Fortunately, the gains promised by the optimal trajectory are great enough that the advantage should be retained even if the trajectory can only be approximated. Future work should further generalization of  $hA$ , possibly by including temperature and/or velocity dependence. Future studies should also look into issues of practical implementation and experimental validation.

## 6 Acknowledgments

Support for this research comes from the National Science Foundation under grant number NSF/EFRI-1038294, the University of Minnesota - Initiative for Renewable Energy and the Environment under project number RS-0027-11, and the Center for Compact and Efficient Fluid Power, a National Science Foundation Engineering Research Center funded under cooperative agreement number EEC-0540834.

## REFERENCES

- [1] Li, P. Y., Van de Ven, J. D., and Sancken, C. J., 2007. "Open accumulator concept for compact fluid power energy storage". In Proceedings of the 2007 ASME-IMEC, no. IMECE2007-42580, ASME.
- [2] Otis, D., 1973. "Thermal losses in gas-charged hydraulic accumulators". In Proceedings of the AIAA 8th Intersociety Energy Conversion Engineering Conference, pp. 198–201.
- [3] Sherman, M. P., and Karlekar, B. V., 1973. "Improving the energy storage capacity of hydraulic accumulators". In Proceedings of the AIAA 8th Intersociety Energy Conversion Engineering Conference, pp. 202–207.
- [4] Sozen, M., and Kuzay, T. M., 1996. "Enhanced heat transfer in round tubes with porous inserts". *Int. J. Heat and Fluid Flow*, **17**(2), pp. 124–129.
- [5] Van de Ven, J. D., and Li, P. Y., 2009. "Liquid piston gas compression". *Applied Energy*, **86**(10), pp. 2183–2191.
- [6] Lewins, J. D., 2003. "Optimising and intercooled compressor for an ideal gas model". *Int. J. Mech. Engr. Educ.*, **31**(3), pp. 189–200.
- [7] Band, Y. B., Kafri, O., and Salamon, P., 1980. "Maximum work production from a heated gas in a cylinder with piston". *Chemical Physical Letters*, **72**(1), May, pp. 127–130.
- [8] Salamon, P., Band, Y. B., and Kafri, O., 1982. "Maximum power from a cycling working fluid". *J. Appl. Physics*, **53**(1), January, pp. 197–202.
- [9] Band, Y. B., Kafri, O., and Salamon, P., 1982. "Finite time thermodynamics: optimal expansion of a heated working fluid". *J. Appl. Physics*, **53**(1), January, pp. 8–28.
- [10] Mozurkewich, M., and Berry, R. S., 1981. "Finite-time thermodynamics: engine performance improved by optimized piston motion". In Proceedings of the National Academy of Sciences, USA, Vol. 78, pp. 1986–1988.
- [11] Hoffman, K. H., Watowich, S. J., and Berry, R. S., 1985. "Optimal paths for thermodynamic systems: the ideal diesel cycle". *J. Appl. Physics*, **58**(6), September, pp. 2125–2134.
- [12] Sancken, C. J., and Li, P. Y., 2009. "Optimal efficiency-power relationship for an air motor-compressor in an energy storage and regeneration system". In Proceedings of the ASME 2009 Dynamic Systems and Control Conference.
- [13] Pourmovahed, A., and Otis, D. R., 1984. "The effects of thermal damping on the dynamic response of a hydraulic motor-accumulator system". *J. Dynamic Systems, Measurement and Control*, **106**(1), pp. 21–26.
- [14] Otis, D. R., and Pourmovahed, A., 1985. "An algorithm for computing nonflow gas processes in hydropneumatic accumulators". *J. Dynamic Systems, Measurement and Control*, **107**(1), pp. 93–96.
- [15] Woschni, G., 1967. "A universally applicable equation for the instantaneous heat transfer coefficient in the internal combustion engine". *SAE Trans.*, **76**, paper 670931.
- [16] Faulkner, H. B., and Smith, J. L., 1983. "Instantaneous heat transfer during compression and expansion in reciprocating gas handling machinery". In Proceedings of the AIAA 18th Intersociety Energy Conversion Engineering Conference, pp. 724–730.
- [17] Polman, J., 1981. "Heat transfer in a piston-cylinder system". *Int. J. Heat Mass Transfer*, **24**(1), pp. 184–187.
- [18] Tabaczynski, R. J., Hoult, D. P., and Keck, J. C., 1970. "High Reynolds number flow in a moving corner". *J. Fluid Mech.*, **42**, pp. 249–255.
- [19] Nikanjam, M., and Greif, R., 1978. "Heat transfer during piston compression". *J. Heat Transfer*, **100**, August, pp. 527–530.
- [20] Greif, R., Namba, T., and Nikanjam, M., 1979. "Heat transfer during piston compression including sidewall and convection effects". *Int. J. Heat Mass Transfer*, **22**, pp. 901–907.
- [21] Hsieh, W. W., and Wu, T. T., 1996. "Experimental investigation of heat transfer in a high-pressure reciprocating gas compressor". *Experimental Thermal and Fluid Sciences*, **13**(1), pp. 44–54.